RESEARCH PAPER

ABILITY TO INHIBIT NO PRODUCTION ON RAW 264.7 CELLS AND α-GLUCOSIDASE ACTIVITY OF APIGENIN-C-GLUCOSIDE-RICH EXTRACT FROM CLINACANTHUS NUTANS IN DIFFERENT ECOLOGICAL REGIONS

Che Thi Cam Ha[1*], Phan Thi Nhu Y[1], Cao Thi Long[2], Nguyen Vinh Phu[2], Phan Duy An[3], Pham Nguyen Cuong[3], Nguyen Thi Minh Thi[4]

[1]University of Sciences, Hue University, Vietnam
[2]Hue University of Medicine and Pharmacy, Hue University
[3]Hue Central Hospital, Vietnam
[4]Graduated student at Université Paris Cité, France
Email:chethicamha@hueuni.edu.vn, chethicamha@husc.edu.vn

Abstract

Clinacanthus nutans is a medicinal plant known to contain various secondary metabolites and exhibit a wide range of biological activities. This study compared *C. nutans* leaf samples collected from hilly and coastal areas of Hue City in terms of leaf anatomy, phytochemical composition, and selected biological activities of their 70% ethanol extracts. The hilly samples had a more developed palisade mesophyll and a higher palisade-to-spongy mesophyll ratio than the coastal samples. They also contained higher levels of total polyphenols, total flavonoids, and vitexin, with corresponding values of 54.6 versus 48.9 mg GAE/g extract, 30.2 versus 26.9 mg QE/g extract, and 11.8 versus 9.6 mg/g extract, respectively. Consistent with these phytochemical differences, the hilly extracts exhibited stronger DPPH radical-scavenging activity, greater inhibitory effects on nitric oxide production and α-glucosidase activity, and more pronounced reductions in TNF-α, IL-6, and IL-1β levels than the coastal extracts. Overall, the hilly-area samples showed a more favorable quality profile, as reflected by their anatomical features, phytochemical contents, and biological activities. These findings provide a scientific basis for selecting suitable *C. nutans* raw materials according to harvesting location.

Keywords: *Clinacanthus nutans*; leaf anatomy; vitexin; antioxidant activity; anti-inflammatory activity; α-glucosidase inhibition

How to cite this article: Ha CTC, Y PTN, Long CT, Phu NV, An PD, Cuong PN, Thi NTM. Ability to inhibit NO production on RAW 264.7 cells and α-glucosidase activity of apigenin-C-glucoside-rich extract from Clinacanthus nutans in different ecological regions. Int J Drug Deliv Technol. 2026;16(75s): 395-402. DOI: 10.25258/ijddt.16.75s.43

1. Introduction

Clinacanthus nutans (Burm. f.) Lindau is a medicinal plant widely used in Southeast Asia and has attracted considerable attention because of its diverse bioactive secondary metabolites, particularly polyphenols, flavonoids, and C-glycosyl flavones such as vitexin [1], [2], [4]. Previous studies have shown that this species exhibits various biological properties, notably antioxidant, anti-inflammatory, and metabolism-regulating effects [1], [2].

In plants, growing conditions can influence leaf structure and the accumulation of secondary metabolites, thereby affecting the chemical quality and biological activities of plant raw materials [13], [14]. However, most studies on *C. nutans* have focused on individual aspects, such as chemical composition or specific biological activities [1]–[12]. Comprehensive studies evaluating the relationships among leaf anatomical characteristics, phytochemical composition, and biological activity in samples collected under different ecological conditions remain limited [1]–[14].

On this basis, the present study compared *C. nutans* samples collected from hilly and coastal areas of Hue City using three groups of criteria: leaf anatomical characteristics; the contents of total polyphenols, total flavonoids, and vitexin; and selected in vitro biological activities, including DPPH radical-scavenging activity, anti-inflammatory activity in an LPS-stimulated RAW 264.7 cell model, and α-glucosidase inhibitory activity. The findings are expected to help clarify ecological variation associated with the collection sites of *C. nutans* and provide an additional scientific basis for selecting appropriate raw material sources [1]–[14].

2. Materials and methodology

2.1. Plant materials and sampling design

Leaves of *Clinacanthus nutans* were collected from two representative areas in Hue City: the hilly region of Binh Thanh Commune and the coastal region of Hai Duong Commune, from March to May 2025. In each area, three independent sampling sites were selected, and at each site, leaves from three mature, healthy plants were collected separately as independent biological samples. Fresh leaves were washed, dried to constant weight at low temperature, ground into powder, and stored for subsequent analyses. The plant

material was taxonomically identified according to published references [1], [2], deposited at the Faculty of Biology, University of Sciences, Hue University, and authenticated by M.Sc. Nguyen Viet Thang.

2.2. Chemicals, reagents, and equipment

Chemicals and reference standards were obtained from Sigma-Aldrich and Merck. Mouse ELISA kits for the quantification of TNF-α, IL-6, and IL-1β were used, with catalog numbers RAB0477, RAB0308, and RAB0274, respectively. UV–Vis analysis was performed using a LABTRONIC LT-39 spectrophotometer, whereas HPLC–DAD analysis was conducted on an Agilent Technologies Series 1200 HPLC system equipped with a DAD detector and ChemStation software. Leaf cross-sections were prepared using a Leica RM2125 microtome, and the stained slides were observed under an Olympus BX51 light microscope.

2.3. Preparation of extracts

Dry leaf powder from each biological sample was extracted separately with 70% ethanol at a plant material-to-solvent ratio of 1:10 (w/v) by maceration at 120 rpm and 28 ± 2°C for 24 h. The extraction procedure was repeated three times to ensure exhaustive recovery of soluble compounds. The extracts were filtered through Whatman No. 1 filter paper, pooled, and concentrated under reduced pressure at 40°C using a rotary evaporator, followed by freeze-drying to obtain the crude extract. The crude extracts were stored at 4°C until use. The extraction yield was calculated using the following equation:

$$\text{Extraction yield (\%)} = \frac{W_1}{W_0} \times 100$$

where W_0 is the initial weight of the dry leaf powder and W_1 is the weight of the crude extract obtained.

2.4. Leaf anatomical analysis

Leaf anatomical features were examined using cross-sections taken from the middle region of the leaf blade. Fresh leaves were fixed in FAA solution for 24 h, dehydrated through a graded ethanol series (50%, 70%, 95%, and 100%), sectioned into thin slices of 8–15 µm, stained with 1% safranin and 0.1% fast green, and mounted in 50% glycerol. The sections were observed under a light microscope at a magnification of 10 × 40. For each sample, three leaves were used; each leaf was sectioned three times, and three sections were prepared from each cut. Images were captured and analyzed using ImageJ software. The measured parameters included the thicknesses of the upper epidermis, palisade mesophyll, spongy mesophyll, lower epidermis, and total leaf blade, as well as the palisade-to-spongy mesophyll ratio.

2.5. Determination of total polyphenol content (TPC)

The total polyphenol content (TPC) of *Clinacanthus nutans* extracts was determined using the Folin–Ciocalteu method [1], [2], [5]. Briefly, 100 µL of the sample solution was mixed with 500 µL of 10% Folin–Ciocalteu reagent and 400 µL of 7.5% Na_2CO_3 solution, and the mixture was then incubated in the dark at room temperature for 30 min. The absorbance was measured at 765 nm. Gallic acid was used as the standard, and the calibration curve was prepared over a concentration range of 0–100 µg/mL, with the regression equation y = ax + b. The results were expressed as mg gallic acid equivalents per gram of extract (mg GAE/g extract). TPC was calculated using the following equation:

$$\text{TPC} = \frac{C \times V \times D}{m}$$

where C is the concentration determined from the calibration curve (mg/mL), V is the volume of the sample solution (mL), D is the dilution factor, and m is the mass of extract used (g).

2.6. Determination of total flavonoid content (TFC)

The total flavonoid content (TFC) of *Clinacanthus nutans* extracts was determined using the aluminum chloride complexation method [1], [2], [5]. Briefly, 500 µL of the sample solution was mixed with 500 µL of 2% $AlCl_3$ solution, incubated at room temperature for 30 min, and the absorbance was measured at 415 nm. Quercetin was used as the standard, and the calibration curve was prepared over a concentration range of 0–100 µg/mL, with the regression equation y = ax + b. The results were expressed as mg quercetin equivalents per gram of extract (mg QE/g extract). TFC was calculated using the same equation as that used for TPC.

2.7. Quantification of vitexin by HPLC–DAD

Vitexin in *Clinacanthus nutans* extracts was quantified using an Agilent Technologies Series 1200 HPLC system coupled with a DAD detector and ChemStation software (Agilent, USA). The samples were dissolved in HPLC-grade methanol and filtered through a 0.45 µm membrane before analysis. Chromatographic separation was performed on a SunFire™ C18 column (250 × 4.6 mm, 5 µm) maintained at 30°C. The mobile phase consisted of acetonitrile (A) and water containing 1% acetic acid (B), with a gradient elution starting at an A:B ratio of 1:9. The flow rate was 1.0 mL/min, the injection volume was 20 µL, and detection was performed at 342 nm. Vitexin was identified by comparing its retention time and UV spectrum with those of the reference standard and was quantified using a calibration curve over a concentration range of 2–25 ppm. The results were expressed as mg/g dry extract.

2.8. Evaluation of DPPH radical scavenging activity

Antioxidant activity was evaluated using the DPPH radical-scavenging assay. Sample solutions at concentrations of 20–100 µg/mL were mixed with 0.1 mM DPPH solution in methanol at a ratio of 1:1 (v/v), incubated in the dark at room temperature for 30 min, and the absorbance was measured at 517 nm. Trolox was used as the positive control. The percentage of

DPPH radical-scavenging activity was calculated using the following equation:

$$\%\text{ức chế} = \frac{A_{control} - (A_{sample} - A_{blank})}{A_{control}} \times 100$$

where $A_{control}$ is the absorbance of the control containing DPPH without the sample, A_{sample} is the absorbance of the reaction mixture containing the sample and DPPH, and A_blank is the absorbance of the sample blank without DPPH. The IC_{50} value was calculated using TableCurve 2Dv4 software.

2.9. RAW 264.7 cell culture

Murine macrophage RAW 264.7 cells were cultured in DMEM supplemented with 10% fetal bovine serum and 1% penicillin–streptomycin at 37°C in a humidified atmosphere containing 5% CO_2. Cells were subcultured when they reached approximately 70–80% confluence.

2.10. Evaluation of cytotoxicity by MTT assay

For the MTT assay, RAW 264.7 cells were seeded in 96-well plates at a density of 1×10^4 cells/well and incubated for 24 h before treatment. The extracts were tested over a concentration range of 3.125–400 µg/mL for 24 h, with DMSO (< 0.1%) used as the solvent control. After treatment, 10 µL of MTT solution (5 mg/mL) was added to each well, followed by incubation for an additional 4 h. The formazan crystals were dissolved in DMSO, and the absorbance was measured at 570 nm. Cell viability was calculated using the following equation:

$$\text{Cell viability } (\%) = \frac{A_1}{A_0} \times 100$$

where A_1 is the absorbance of the treated sample, and A_0 is the absorbance of the solvent control group.

2.11. Evaluation of anti-inflammatory activity through nitric oxide (NO) inhibition

RAW 264.7 cells were seeded in 96-well plates at a density of 1×10^5 cells/well, incubated for 24 h, and then co-treated with the extracts at concentrations of 3.125–100 µg/mL and LPS at 1 µg/mL for 24 h. The experimental groups included the negative control (untreated cells), solvent control, LPS-treated group, extract + LPS groups, and dexamethasone + LPS group. Dexamethasone, at concentrations of 100, 50, 25, 12.5, 6.25, and 3.125 µM, was used as the positive control.

NO concentration in the culture supernatant was indirectly determined using Griess reagent. Briefly, 100 µL of the supernatant was mixed with 100 µL of Griess reagent, incubated for 10 min at room temperature, and the absorbance was measured at 540 nm. Sodium nitrite was used to construct a standard curve over a concentration range of 0–100 µM. The percentage inhibition of NO production was calculated using the following equation:

$$\%\text{ NO inhibition } = \frac{A_{LPS} - A_{sample}}{A_{LPS} - A_{blank}} \times 100$$

Where A_{LPS} is the absorbance of the LPS-treated group only, A_{sample} is the absorbance of the sample-treated group in the presence of LPS and A_{blank} is the absorbance of the untreated control group without LPS. The IC_{50} value was determined using TableCurve 2Dv4 software.

2.12. Quantification of TNF-α, IL-6, and IL-1β by ELISA

Culture supernatants collected after 24 h of co-treatment of RAW 264.7 cells with the extracts and LPS were used to quantify TNF-α, IL-6, and IL-1β using mouse-specific ELISA kits from Merck/Sigma-Aldrich, with catalog numbers RAB0477, RAB0308, and RAB0274, respectively. The absorbance was measured at 450 nm, cytokine concentrations were calculated from the corresponding standard curves, and the results were expressed as percentages relative to the LPS-treated group.

2.13. Evaluation of α-glucosidase inhibitory activity

α-glucosidase inhibitory activity was determined using a colorimetric method with p-nitrophenyl-α-D-glucopyranoside (pNPG) as the substrate. Sample solutions at concentrations of 12.5–200 µg/mL were incubated with α-glucosidase from *Saccharomyces cerevisiae* (0.5 U/mL) in 0.1 M phosphate buffer (pH 6.8) at 37°C for 10 min. Subsequently, 5 mM pNPG was added, and the mixture was further incubated for 20 min. The reaction was terminated by adding 0.2 M Na_2CO_3, and the absorbance was measured at 405 nm. Acarbose was used as the positive control over the same concentration range of 12.5–200 µg/mL. The percentage inhibition was calculated using the following equation:

$$\%\text{inhibition} = \frac{A_0 - A_1}{A_0} \times 100$$

where A_0 is the absorbance of the control without test sample and A_1 is the absorbance of the test sample. The IC_{50} value was determined using a four-parameter logistic (4PL) model with TableCurve 2Dv4 software.

2.14. Statistical analysis

Data were expressed as mean ± SD. Statistical analysis was performed using SPSS; comparisons between two groups were conducted using Welch's t-test, while comparisons among multiple groups were performed using one-way ANOVA followed by Tukey's test. IC_{50} values were determined using TableCurve 2Dv4 software. Differences were considered statistically significant at $p < 0.05$.

3. Results

3.1. Leaf anatomical characteristics

Observation of transverse sections of the leaf blade showed that both groups of *Clinacanthus nutans* samples exhibited a bifacial leaf structure composed of the upper epidermis, palisade mesophyll, spongy mesophyll, and lower epidermis (Figure 1). However, distinct differences between the two groups were

observed in the photosynthetic tissues. Samples from the hilly region displayed a more developed palisade mesophyll, characterized by more elongated and densely arranged cells, whereas samples from the coastal region showed a more developed spongy mesophyll with larger intercellular spaces. Quantitative analysis showed that palisade mesophyll thickness was significantly greater in hilly-region samples than in coastal samples (73.02 ± 4.8 vs. 59.12 ± 3.9 µm; $p < 0.001$). In contrast, spongy mesophyll thickness was significantly greater in coastal samples than in hilly-region samples (70.8 ± 4.3 vs. 61.91 ± 3.8 µm; $p = 0.003$). The palisade-to-spongy mesophyll ratio was also markedly higher in hilly-region samples (1.31 ± 0.08 vs. 0.79 ± 0.07; $p < 0.001$). By contrast, the thicknesses of the upper epidermis, lower epidermis, and total leaf blade did not differ significantly between the two groups ($p > 0.05$) (Table 1).

Table 1. Quantitative anatomical characteristics of *C. nutans* leaves collected from hilly and coastal regions.

Trait	Hilly	Coastal	p-value
Upper epidermis thickness (µm)	17.52 ± 1.4	16.18 ± 1.2	0.214
Palisade mesophyll thickness (µm)	73.02 ± 4.8	59.12 ± 3.9	<0.001
Spongy mesophyll thickness (µm)	61.91 ± 3.8	70.8 ± 4.3	0.003
Lower epidermis thickness (µm)	15.2 ± 1.1	13.92 ± 1.0	0.287
Total leaf thickness (µm)	167.18 ± 6.5	159.36 ± 4.8	0.091
Palisade/spongy ratio	1.31 ± 0.08	0.79 ± 0.07	<0.001

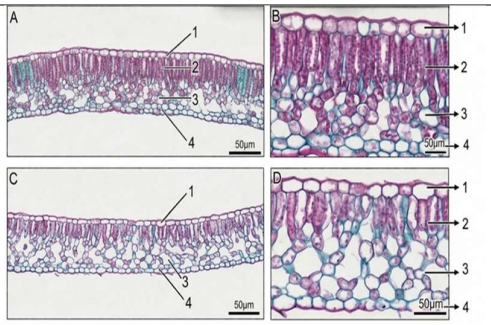

Figure 1. Transverse leaf anatomy of *Clinacanthus nutans* samples from hilly and coastal regions. (A, B) Hilly region; (C, D) coastal region. 1, upper epidermis; 2, palisade mesophyll; 3, spongy mesophyll; 4, lower epidermis.

3.2. Total polyphenol and total flavonoid contents

The analysis showed that *C. nutans* samples collected from the hilly region had higher total polyphenol content (TPC) and total flavonoid content (TFC) than those collected from the coastal region (Figure 2). Specifically, TPC was higher in hilly-region samples than in coastal samples, with values of 54.6 ± 2.1 and 48.9 ± 1.7 mg GAE/g extract, respectively. Similarly, TFC was higher in hilly-region samples than in coastal samples, with values of 30.2 ± 1.3 and 26.9 ± 1.1 mg QE/g extract, respectively. The differences in both parameters were statistically significant ($p < 0.05$). The calibration curves for gallic acid and quercetin both showed good linearity over the tested concentration range, with regression equations of $y = 0.0095x + 0.0205$ ($R^2 = 0.999$) and $y = 0.0076x + 0.0157$ ($R^2 = 0.999$), respectively.

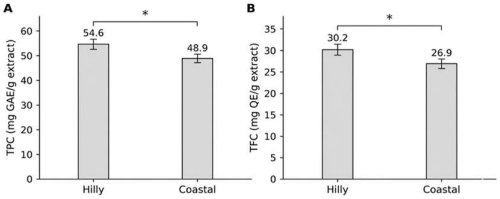

Figure 2. TPC and TFC of *Clinacanthus nutans* samples collected from hilly and coastal regions.

3.3. Vitexin content

HPLC–DAD analysis showed that vitexin was detected in both groups of *C. nutans* samples, with a characteristic peak at a retention time of 20.8 ± 0.1 min, consistent with that of the vitexin standard (Figure 3). Comparison of the chromatograms showed that the vitexin peak area was larger in the hilly-region sample than in the coastal sample. Quantitative analysis showed that vitexin content was significantly higher in hilly-region samples than in coastal samples, with values of 11.8 ± 0.8 and 9.6 ± 0.7 mg/g dry extract, respectively ($p < 0.05$). The calibration curve for vitexin over the concentration range of 2–25 ppm showed good linearity, with the regression equation $y = 15.258x - 12.527$ and a correlation coefficient of $R^2 = 0.9993$.

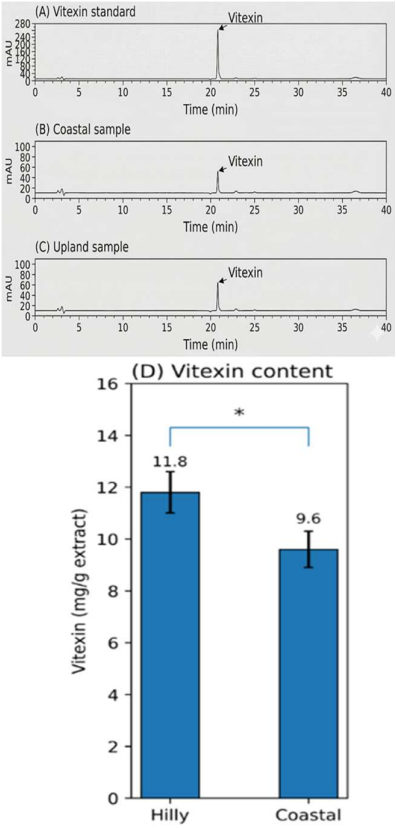

Figure 3. HPLC–DAD chromatograms of vitexin standard and *Clinacanthus nutans* extracts. (A) Vitexin standard; (B) coastal sample; (C) hilly sample.

3.4. DPPH radical scavenging activity

Both *C. nutans* extracts exhibited concentration-dependent DPPH radical-scavenging activity over the concentration range of 20–100 µg/mL (Figure 4). At the same tested concentrations, the hilly-region extract consistently showed a higher percentage of inhibition than the coastal extract. The IC_{50} value of the hilly-region extract was 23.0 ± 1.1 µg/mL, which was significantly lower than that of the coastal extract (28.4 ± 1.3 µg/mL; $p < 0.05$). Trolox, used as the positive control, had an IC_{50} value of 4.46 µg/mL.

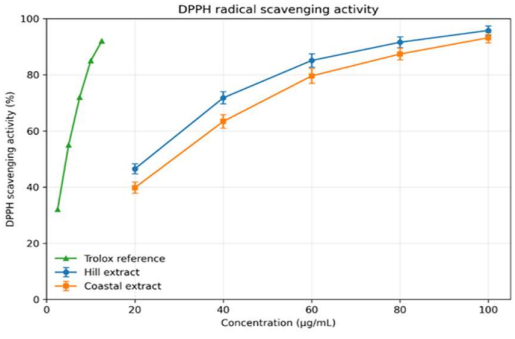

Figure 4. DPPH radical scavenging activity of *C. nutans* extracts from the hilly and coastal regions.

3.5. Cytotoxicity on RAW 264.7 cells

The cytotoxicity of *C. nutans* extracts in RAW 264.7 cells was evaluated using the MTT assay over a concentration range of 3.125–400 µg/mL (Figure 5). Both extracts showed no significant cytotoxicity at concentrations ranging from 3.125 to 100 µg/mL, with cell viability remaining close to that of the solvent control and showing no statistically significant difference ($p > 0.05$). At 200 µg/mL, cell viability slightly decreased to 92.6 ± 4.8% for the hilly-region extract and 91.8 ± 5.0% for the coastal extract. At 400 µg/mL, cell viability further decreased to 85.4 ± 5.5% and 84.7 ± 5.7%, respectively. Based on these results, the concentration range of 3.125–100 µg/mL was selected for subsequent anti-inflammatory experiments.

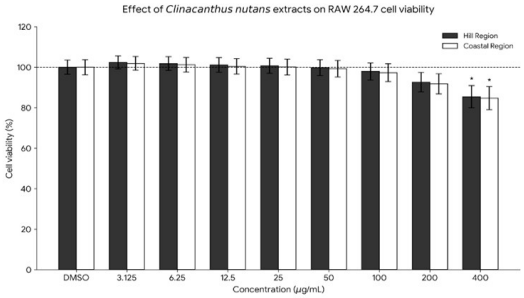

Figure 5. Effects of *Clinacanthus nutans* extracts from the hilly and coastal regions on the viability of RAW 264.7 cells in the MTT assay.

3.6. Inhibition of nitric oxide (NO) production

In the LPS-stimulated RAW 264.7 cell model, both *C. nutans* extracts inhibited NO production in a concentration-dependent manner over a concentration range of 3.125–100 µg/mL (Figure 6). The hilly-region extract showed stronger inhibitory effects than the coastal extract at the same tested concentrations. At 100 µg/mL, NO production inhibition reached 84.7 ± 1.8% for the hilly-region extract and 80.6 ± 1.9% for the coastal extract. The positive control dexamethasone showed stronger inhibition, reaching 91.4 ± 1.7% at 100 µM. The IC_{50} value of the hilly-region extract was 23.1 ± 1.6 µg/mL, which was lower than that of the coastal extract (28.2 ± 1.9 µg/mL). Dexamethasone had an IC_{50} value of 12.79 µM, equivalent to approximately 5.02 µg/mL.

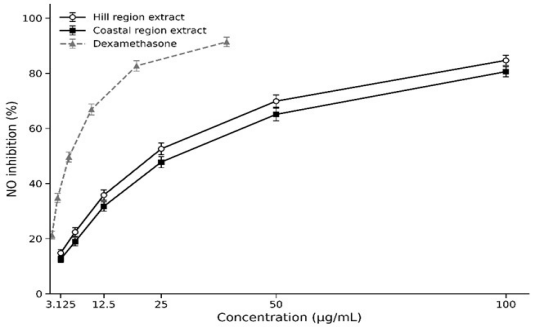

Figure 6. NO inhibitory activity of *Clinacanthus nutans* extracts from hilly and coastal regions in LPS-stimulated RAW 264.7 cells.

3.7. Effects on pro-inflammatory cytokines

To further evaluate the inflammatory response, the effects of *C. nutans* extracts on TNF-α, IL-6, and IL-1β levels were investigated in the LPS-stimulated RAW 264.7 cell model at a concentration of 50 µg/mL. The results showed that LPS treatment markedly increased the levels of all three cytokines, whereas both extracts significantly reduced these inflammatory markers.

In the hilly-region extract + LPS group, TNF-α, IL-6, and IL-1β levels were reduced to 61.7 ± 3.9%, 58.9 ± 4.3%, and 56.8 ± 3.7% of those in the LPS-treated group, respectively. In contrast, in the coastal extract + LPS group, the corresponding values were 70.4 ± 4.6%, 67.8 ± 4.9%, and 65.9 ± 4.2%. Dexamethasone again showed stronger efficacy, with corresponding values of 41.2 ± 3.1%, 39.7 ± 3.4%, and 36.8 ± 3.0% relative to the LPS-treated group.

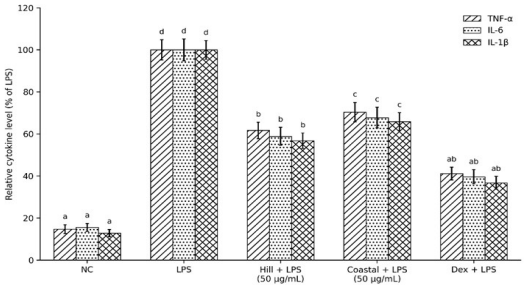

Figure 7. Effects of *Clinacanthus nutans* extracts from hilly and coastal regions on pro-inflammatory cytokine levels in LPS-stimulated RAW 264.7 cells. Bars labeled with different letters indicate statistically significant differences among groups, as determined by one-way ANOVA followed by Tukey's test ($p < 0.05$). NC, negative control; LPS, inflammatory control; Dex, dexamethasone.

3.8. α-glucosidase inhibitory activity

Both *C. nutans* extracts exhibited concentration-dependent α-glucosidase inhibitory activity over the tested concentration range (Figure 8). The hilly-region extract showed stronger activity than the coastal extract, with IC_{50} values of 48.59 ± 3.51 and 63.49 ± 2.24 µg/mL, respectively. The positive control acarbose had an IC_{50} value of 6.26 ± 3.07 µg/mL.

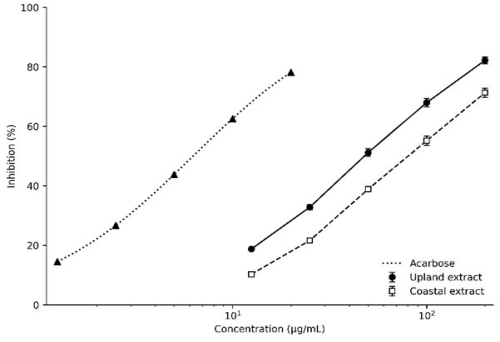

Figure 8. α-Glucosidase inhibitory activity of *Clinacanthus nutans* extracts from hilly and coastal regions as a function of concentration.

4. Discussion

The results of this study showed that differences between the two sources of *Clinacanthus nutans* samples were consistently observed across leaf anatomical features, chemical composition, and biological activities. Samples collected from the hilly area exhibited more developed palisade mesophyll, a higher palisade-to-spongy mesophyll ratio, and greater accumulation of TPC, TFC, and vitexin than those collected from the coastal area. In parallel, extracts from the hilly-area samples showed stronger DPPH radical-scavenging activity, greater inhibition of NO production, more pronounced reductions in TNF-α, IL-6, and IL-1β levels, and stronger α-glucosidase inhibitory activity. The recurrence of the same trend across multiple parameters suggests that the differences between the two sample sources do not represent isolated variation in individual measurements, but rather reflect genuine differences in raw material quality.

At the anatomical level, the main differences were observed in the palisade mesophyll, spongy mesophyll, and palisade-to-spongy mesophyll ratio, whereas the epidermal layers and total leaf thickness did not differ significantly. This pattern of variation indicates that the differences between the two sample sources were primarily associated with the photosynthetic tissue system rather than the overall leaf blade structure. According to Fritz et al. [13], leaf morphology is highly plastic and often reflects plant functional adjustment to differences in growth conditions. In this context, the more developed palisade mesophyll observed in hilly-area samples may suggest greater photosynthetic and metabolic capacity, thereby creating more favorable conditions for the accumulation of secondary metabolites. Therefore, the anatomical findings of the present study are not merely descriptive in terms of morphology, but also provide structural evidence supporting the chemical differences between the two sample sources.

The quantitative results for TPC, TFC, and vitexin further support this interpretation. Previous studies have reported that *C. nutans* is rich in polyphenols, flavonoids, and flavone C-glycosides, among which vitexin is considered a notable marker compound [1], [2], [4]. In the present study, both general indicators, such as TPC and TFC, and the more specific indicator vitexin were higher in hilly-area samples. This suggests that differences in raw material source were reflected not only in the general accumulation of phenolic compounds, but also in a specific chemical marker. Compared with studies focusing solely on compound identification or quantification, the present findings are more informative because they place these chemical indicators in direct relation to anatomical characteristics and biological responses, thereby clarifying their value in raw material quality assessment.

The relationship between chemical composition and antioxidant activity was also evident in this study. Hilly-area samples contained higher levels of TPC,

TFC, and vitexin and exhibited a lower DPPH IC_{50} value than coastal samples. This finding is consistent with previous reports showing that the antioxidant activity of *C. nutans* is closely associated with its phenolic and flavonoid composition [1], [2], [5]. Thus, in this study, the DPPH assay not only confirmed the antioxidant activity of the extracts, but also demonstrated that the magnitude of this activity varied in parallel with the chemical markers between the two sample sources. This finding supports the value of the assay for stratifying raw material quality, particularly when interpreted together with anatomical and chemical parameters.

A similar trend was observed in the anti-inflammatory model. Both extracts inhibited NO production in LPS-stimulated RAW 264.7 cells, but the hilly-area extracts showed stronger effects, as reflected by lower IC_{50} values and greater reductions in TNF-α, IL-6, and IL-1β levels. Notably, this difference was not limited to a single inflammatory marker, but was consistently observed across multiple inflammation-related parameters. This consistency strengthens the interpretation of the anti-inflammatory activity. Previous studies have likewise shown that *C. nutans* can modulate NO production and cytokine responses in macrophage models [6], [8], [9]. In the present study, the fact that hilly-area samples were simultaneously richer in TPC, TFC, and vitexin suggests that a more favorable chemical profile may provide an important basis for explaining the stronger anti-inflammatory efficacy of this sample source. In addition, the MTT results showed that the concentrations used in the experiments did not significantly reduce RAW 264.7 cell viability; therefore, the observed decreases in NO and cytokine levels most likely reflect genuine anti-inflammatory modulation by the extracts.

Regarding α-glucosidase inhibitory activity, the hilly-area extracts again showed stronger efficacy than the coastal extracts. This result is consistent with the overall trend observed for the other chemical and biological parameters. Previous studies have shown that vitexin is capable of inhibiting α-glucosidase and that flavonoids in general also have the potential to modulate this enzyme [11], [12]. Therefore, the higher TFC and vitexin contents in hilly-area samples provide a reasonable basis for explaining their lower α-glucosidase IC_{50} values. Although this activity cannot yet be attributed to a single specific compound, the results still indicate that differences in the flavonoid profile between the two sample sources are accompanied by clear differences in metabolic regulatory potential. This broadens the value of *C. nutans* raw material evaluation, not only from the perspective of antioxidant or anti-inflammatory activity, but also in terms of another functional property with potential practical relevance.

When the results are considered as a whole, the hilly-area samples demonstrated advantages across three levels of evidence: leaf structure, chemical markers, and biological functional responses. This consistency gives the study its significance for raw material evaluation. Rather than merely describing a single group of parameters, the study shows that the sample source with more developed palisade mesophyll was also the source that accumulated phenolic compounds, flavonoids, and vitexin more effectively and, at the same time, exhibited stronger biological activities. On this basis, it can be concluded that *C. nutans* samples from the hilly area displayed a more favorable quality profile than those from the coastal area under the investigated conditions. These findings provide additional experimental support for the selection of cultivation or harvesting areas and demonstrate the value of an integrated anatomical, chemical, and biological approach to the standardization of medicinal plant materials.

Conclusion

This study demonstrated that *Clinacanthus nutans* samples collected from hilly and coastal areas exhibited clear differences in leaf anatomical characteristics, phytochemical composition, and biological activities. Samples from the hilly area showed more developed palisade mesophyll, a higher palisade-to-spongy mesophyll ratio, and greater accumulation of TPC, TFC, and vitexin than those from the coastal area. In addition, extracts from the hilly area exhibited stronger antioxidant, anti-inflammatory, and α-glucosidase inhibitory activities. The consistency among anatomical, chemical, and biological parameters indicates that samples from the hilly area represent a higher-quality raw material source than those from the coastal area. These findings not only provide practical evidence for the selection of *C. nutans* raw materials according to harvesting region, but also highlight the value of integrating leaf anatomical traits, phytochemical markers, and biological activities in the evaluation and standardization of medicinal plant materials.

Acknowledgments: This research was financially supported by the Hue University Research Project, Grant No. DHH2025-01-222.

References

[1] Kamarudin, M. N. A., Sarker, M. M. R., Kadir, H. A., & Ming, L. C. (2017). Ethnopharmacological uses, phytochemistry, biological activities, and therapeutic applications of Clinacanthus nutans (Burm. f.) Lindau: A comprehensive review. *Journal of ethnopharmacology*, *206*, 245–266. https://doi.org/10.1016/j.jep.2017.05.007

[2] Chia, T. Y., Gan, C. Y., Murugaiyah, V., Hashmi, S. F., Fatima, T., Ibrahim, L., Abdulla, M. H., Alswailmi, F. K., Johns, E. J., & Ahmad, A. (2021). A Narrative Review on the Phytochemistry, Pharmacology and Therapeutic Potentials of *Clinacanthus nutans* (Burm. f.) Lindau Leaves as an Alternative Source of Future Medicine. *Molecules (Basel, Switzerland)*, *27*(1), 139. https://doi.org/10.3390/molecules27010139

[3] Chiangchin, S., Thongyim, S., Pandith, H., Kaewkod, T., Tragoolpua, Y., Inta, A., Watthana, S., Pongamornkul, W., Jangsutthivorawat, S., & Panya, A. (2023). Clinacanthus nutans genetic diversity and its association with anti-apoptotic, antioxidant, and anti-bacterial activities. *Scientific reports*, *13*(1), 19566. https://doi.org/10.1038/s41598-023-46105-z

[4] Chelyn, J. L., Omar, M. H., Mohd Yousof, N. S., Ranggasamy, R., Wasiman, M. I., & Ismail, Z. (2014). Analysis of flavone C-glycosides in the leaves of Clinacanthus nutans (Burm. f.) Lindau by HPTLC and HPLC-UV/DAD. *TheScientificWorldJournal*, *2014*, 724267. https://doi.org/10.1155/2014/724267

[5] Ismail, N. Z., Md Toha, Z., Muhamad, M., Nik Mohamed Kamal, N. N. S., Mohamad Zain, N. N., & Arsad, H. (2020). Antioxidant Effects, Antiproliferative Effects, and Molecular Docking of *Clinacanthus nutans* Leaf Extracts. *Molecules (Basel, Switzerland)*, *25*(9), 2067. https://doi.org/10.3390/molecules25092067

[6] Khoo, Leng Wei & Kow, Audrey & M., Maulidiani & Ang, May & Chew, Won & Lee, Ming Tatt & Tan, Chin & Tham, Chau & Abas, Faridah. (2018). 1 H-NMR metabolomics for evaluating the protective effect of Clinacanthus nutans (Burm. f) Lindau water extract against nitric oxide production in LPS-IFN- γ activated RAW 264.7 macrophages. Phytochemical Analysis. 30. 10.1002/pca.2789

[7] Kow, A. S. F., Khoo, L. W., Tan, J. W., Abas, F., Lee, M. T., Israf, D. A., Shaari, K., & Tham, C. L. (2023). Clinacanthus nutans aqueous leaves extract exerts anti-allergic activity in preclinical anaphylactic models via alternative IgG pathway. *Journal of ethnopharmacology*, *303*, 116003. https://doi.org/10.1016/j.jep.2022.116003

[8] Mohamed, Nur & Lim, Vuanghao & Mohamed, Rafeezul & Ismail, Ida. (2022). Regulation of the Macrophage Cellular Response by Clinacanthus nutans Extracts in J774.2 Macrophages. Journal of Herbal Medicine. 33. 100558. 10.1016/j.hermed.2022.100558

[9] Ong, W. Y., Herr, D. R., Sun, G. Y., & Lin, T. N. (2022). Anti-Inflammatory Effects of Phytochemical Components of *Clinacanthus nutans*. *Molecules (Basel, Switzerland)*, *27*(11), 3607. https://doi.org/10.3390/molecules27113607

[10] Ban, W. K., Fong, I. L., Khong, H. Y., & Phung, J. H. Y. (2022). Wound Healing, Antimicrobial and Antioxidant Properties of *Clinacanthus nutans* (Burm.f.) *Lindau* and *Strobilanthes crispus* (L.) *Blume* Extracts. *Molecules*, *27*(5), 1722. https://doi.org/10.3390/molecules27051722

[11] Ni, Mengting & Hu, Xing & Gong, Deming & Zhang, Guowen. (2020). Inhibitory mechanism of vitexin on α-glucosidase and its synergy with acarbose. Food Hydrocolloids. 105. 105824. 10.1016/j.foodhyd.2020.105824.

[12] Şöhretoğlu, D., Sari, S. Flavonoids as alpha-glucosidase inhibitors: mechanistic approaches merged with enzyme kinetics and molecular modelling. *Phytochem Rev* **19**, 1081–1092 (2020). https://doi.org/10.1007/s11101-019-09610-6

[13] Fritz, M. A., Rosa, S., & Sicard, A. (2018). Mechanisms Underlying the Environmentally Induced Plasticity of Leaf Morphology. *Frontiers in genetics*, *9*, 478. https://doi.org/10.3389/fgene.2018.00478

[14] Vinogradova, N., Vinogradova, E., Chaplygin, V., Mandzhieva, S., Kumar, P., Rajput, V. D., Minkina, T., Seth, C. S., Burachevskaya, M., Lysenko, D., & Singh, R. K. (2023). Phenolic Compounds of the Medicinal Plants in an Anthropogenically Transformed Environment. *Molecules (Basel, Switzerland)*, *28*(17), 6322. https://doi.org/10.3390/molecules28176322

[15] Daglia M. (2012). Polyphenols as antimicrobial agents. *Current opinion in biotechnology*, *23*(2), 174–181. https://doi.org/10.1016/j.copbio.2011.08.007